

## Acute paracetamol-induced hepatotoxicity in Wistar rats: biochemical and histopathological evaluation and the hepatoprotective effect of *Silybum marianum* (L.) Gaertn.

Asma Fraia<sup>1,\*</sup>, Wafa Habbachi<sup>2</sup>, and Hacène Frih<sup>1</sup>

<sup>1</sup>Environmental Biosurveillance Laboratory, Badji Mokhtar-Annaba University 12, P.O. Box 23000 Annaba, Algeria

<sup>2</sup>Applied Neuroendocrinology Laboratory, Badji Mokhtar-Annaba University 12, P.O.Box 23000 Annaba, Algeria

\*Corresponding author: asma.fraia@univ-annaba.dz

Received: April 17, 2026; Revised: May 13, 2026; Accepted: May 15, 2026; Published online: May 20, 2026

**Abstract:** Paracetamol administration at hepatotoxic doses represents a widely used experimental model to investigate drug-induced liver injury, causing significant hepatic damage through the generation of reactive metabolites that deplete glutathione and trigger oxidative stress, without necessarily causing mortality. This study evaluated the hepatotoxic effects of acute paracetamol administration and the hepatoprotective potential of *Silybum marianum* in Wistar rats. Biochemical markers (alanine aminotransferase, aspartate aminotransferase, alkaline phosphatase, and bilirubin) and liver histopathology were examined. Paracetamol induced marked histological liver damage, including hepatocellular necrosis and architectural disorganization, with only moderate and inconsistent changes in serum enzyme levels, indicating a dissociation between biochemical markers and structural hepatic injury. *S. marianum* treatment improved liver histology and partially stabilized biochemical alterations, supporting its hepatoprotective activity through antioxidant and membrane-stabilizing mechanisms. These results show that histopathological examination is a more sensitive indicator of acute hepatic injury than serum transaminases and support the therapeutic potential of *S. marianum* in paracetamol-induced hepatotoxicity.

**Keywords:** paracetamol, hepatotoxicity, *Silybum marianum*, hepatoprotection, oxidative stress

### INTRODUCTION

The liver is the primary organ responsible for xenobiotic biotransformation and is consequently highly susceptible to drug-induced injury. Among the various mechanisms implicated in hepatotoxicity, oxidative stress, mitochondrial dysfunction, and inflammatory signaling play central roles in the progression of hepatocellular damage [1-3].

Paracetamol (acetaminophen) is one of the most widely used analgesic and antipyretic agents worldwide [4,5]. At therapeutic doses, it is considered safe; however, administration at hepatotoxic doses leads to significant liver injury without necessarily causing mortality, making it a widely used and well-validated experimental model for the study of acute drug-induced liver injury (DILI). Its metabolism involves glucuronidation and sulfation pathways, but a fraction is bioactivated by cytochrome P450 enzymes (mainly CYP2E1, CYP1A2, and CYP3A4) into the highly

reactive metabolite N-acetyl-p-benzoquinone imine (NAPQI). Under physiological conditions, NAPQI is detoxified by hepatic glutathione (GSH). When GSH stores are depleted, NAPQI accumulates, leading to oxidative stress, mitochondrial dysfunction, and hepatocellular necrosis [6-9]. Mechanistically, paracetamol-induced liver injury is characterized by covalent protein adduct formation, lipid peroxidation, mitochondrial permeability transition, and activation of necrotic and inflammatory cell death pathways. Kupffer cell activation and subsequent release of pro-inflammatory cytokines (TNF- $\alpha$ , IL-1 $\beta$ , IL-6) further amplify hepatic damage [9-11].

In recent years, natural products with antioxidant and hepatoprotective properties have gained increasing attention as potential therapeutic strategies against liver injury. Among them, *Silybum marianum* (milk thistle) is one of the most extensively studied medicinal plants. Its active flavonolignan complex, silymarin, exhibits potent antioxidant, anti-inflammatory, and

membrane-stabilizing properties [12-14]. It enhances intracellular glutathione levels, scavenges reactive oxygen species, inhibits lipid peroxidation, and modulates inflammatory signaling pathways, thereby mitigating toxin-induced hepatic injury [12,13,15]. Experimental animal models, particularly Wistar rats, remain essential for elucidating the mechanisms of hepatotoxicity and evaluating hepatoprotective agents because of their physiological and metabolic similarity to humans [16,17]. These models enable the assessment of biochemical markers, including alanine aminotransferase (ALT), aspartate aminotransferase (AST), alkaline phosphatase (ALP), and bilirubin, as well as histopathological changes, providing robust translational relevance to human liver pathophysiology.

Although paracetamol-induced hepatotoxicity has been extensively characterized at biochemical and mechanistic levels, the temporal relationship between circulating biochemical markers and the severity of histopathological liver injury remains incompletely understood in acute experimental settings. In particular, moderate or inconsistent alterations in serum biomarkers may not always accurately reflect the extent of underlying structural hepatic damage. Furthermore, while the hepatoprotective properties of *S. marianum* are well documented, its ability to preserve liver histoarchitecture independently of full biochemical normalization under acute toxic conditions remains insufficiently explored. This raises the important question of whether histopathological assessment may reveal protective effects of *S. marianum* that are only partially reflected by conventional serum biomarkers. We therefore hypothesized that acute paracetamol exposure would induce marked structural liver injury accompanied by moderate biochemical disturbances, and that treatment with *S. marianum* would attenuate hepatic damage through antioxidant, anti-inflammatory, and membrane-stabilizing mechanisms.

The present study aimed to evaluate the hepatotoxic effects of acute paracetamol administration in Wistar rats through integrated biochemical and histopathological analyses. It further investigated the roles of oxidative stress and inflammatory processes in the observed hepatic alterations and assessed the hepatoprotective potential of *S. marianum* in mitigating paracetamol-induced liver damage.

## MATERIALS AND METHODS

### Ethics statement

All procedures involving animals were conducted in strict accordance with the guidelines for the care and use of laboratory animals of the Algerian Institutional Ethical Committee for Animal Research under agreement number 45/DGLPAG/DVA/SDA/14, issued by the General Directorate of Agricultural and Genetic Production Laboratories, Directorate of Veterinary Services, and Sub-Directorate of Animal Health on December 18, 2014.

### Chemicals

Paracetamol (N-acetyl-p-aminophenol;  $C_8H_9NO_2$ ) was used as a reference hepatotoxic agent. It is a widely prescribed non-salicylate analgesic and antipyretic [4-6,16]. At therapeutic doses, paracetamol is considered safe; however, at high doses, it is known to induce acute liver injury through the formation of the reactive metabolite N-acetyl-p-benzoquinone imine [4-6,16]. Paracetamol (acetaminophen) used in this study was of pharmaceutical grade and prepared freshly prior to administration.

### Plant identification and extraction

*Silybum marianum* (L.) Gaertn. (milk thistle) belongs to the Asteraceae family and is widely distributed throughout the Mediterranean Basin and North America. Approximately 1.5 m in height, it is characterized by its spiny leaves marbled with white and its intensely pink flowers [12,13]. It is well known for its hepatoprotective, antioxidant, anti-inflammatory, and liver-regenerative properties, and is widely used in both traditional and clinical settings for the management of hepatic, digestive, and metabolic disorders, as well as certain cardiovascular and neurodegenerative conditions [12-15,18,37,42]. Fresh preparations were made daily.

An aqueous extract of *S. marianum* seeds was prepared by infusion. The seeds were obtained from a local herbal supplier and authenticated on the basis of their botanical characteristics. The plant material was identified by Prof. Rebbas Khellaf, a taxonomist in the Department of Biology, University of M'sila, Algeria (No. KR0197). In accordance with traditional

phytotherapeutic practices, the infusion was prepared by adding 50 g of whole seeds to 1 L of boiling water and steeping for 10-15 min. The solution was then filtered and allowed to cool before administration. Fresh preparations were made daily throughout the treatment period.

### Animals and experimental design

Adult male Wistar rats (24) weighing 200-250 g were obtained from the Pasteur Institute of Algiers. Animals were housed in the animal facility of Badji Mokhtar University of Annaba (UBMA, Algeria) under controlled environmental conditions (temperature  $22\pm 2^{\circ}\text{C}$ ; relative humidity 45-55%; 12 h light/dark cycle), with ad libitum access to a standard laboratory diet and water. After a 21-day acclimation period, the animals were divided into four groups (n = 6 per group). Control group (G1): animals received a single intraperitoneal (IP) injection of sterile 0.9% NaCl solution (1 mL/100 g body weight) on day 1 and had free access to water throughout the 20-day experimental period. Animals in the paracetamol group (G2) received a single IP injection of paracetamol (450 mg/kg body weight as 45 mg/mL, as 1 mL/100 g) on day 1 and had free access to water for 20 days. In the paracetamol + *S. marianum* group (G3), animals received a single IP injection of paracetamol (450 mg/kg) on day 1, followed by free access to an aqueous herbal infusion of *S. marianum* (50 g/L) from day 2 onwards for 19 consecutive days. *S. marianum* group alone (G4): animals received a single IP injection of 0.9% NaCl on day 1, followed by free access to an aqueous herbal infusion of *S. marianum* (50 g/L) from day 2 onwards for 19 consecutive days.

Hepatotoxicity was induced by a single intraperitoneal injection of paracetamol (450 mg/kg body weight), a well-established and widely validated model of acute liver injury in rodents that does not induce mortality. Paracetamol was prepared extemporaneously in sterile 0.9% NaCl solution prewarmed to  $37^{\circ}\text{C}$  to facilitate dissolution and ensure homogeneity. The solution was prepared immediately before administration to guarantee stability and dosing accuracy. Individual doses were adjusted according to body weight and administered intraperitoneally under aseptic conditions, with the injection volume standardized at 1 mL/100 g body weight. Animals were closely monitored following injections for any signs of distress and had free access to

water throughout the experiment. The hepatoprotective treatment consisted of a *S. marianum* aqueous herbal infusion (50 g/L), administered as the sole drinking fluid from day 2 following paracetamol injection, for 19 consecutive days. This administration mode was chosen to reproduce continuous phytotherapeutic exposure under conditions analogous to traditional use. The dose selected was based on previous studies demonstrating the hepatoprotective properties of *S. marianum* extracts.

### Blood sampling and biochemical analysis

Blood samples were collected at three time points: (i) T1, day 1 (24 h post-administration), corresponding to the peak of acute paracetamol-induced hepatotoxicity, when transaminase levels are expected to reach maximal values according to the literature [5,23,29,30]; (ii) T2, day 11 (10 days post-administration), corresponding to the assessment of spontaneous hepatic recovery or recovery supported by *S. marianum*; and (iii) T3, day 21 (20 days post-administration), corresponding to the evaluation of advanced liver regeneration and the experimental endpoint (sacrifice). Blood was collected via retro-orbital puncture into dry tubes without anticoagulant. Samples were allowed to clot at room temperature and subsequently centrifuged at 3,000 rpm for 10 min at  $4^{\circ}\text{C}$  to obtain serum, which was stored at  $-20^{\circ}\text{C}$  until biochemical analysis.

Serum samples were used to obtain biochemical parameters analysis, including alanine aminotransferase (ALT), aspartate aminotransferase (AST), alkaline phosphatase (ALP), total bilirubin (TB) and direct bilirubin (DB). The activities of those were determined using standard spectrophotometric methods with commercially available diagnostic kits, according to the manufacturers' instructions.

### ALT AND AST ASSAYS

ALT and AST activities were determined according to the Reitman and Frankel method [19]. Briefly, 0.5 mL of substrate solution (containing L-alanine and  $\alpha$ -ketoglutarate for ALT, or L-aspartate and  $\alpha$ -ketoglutarate for AST) was mixed with 0.1 mL of serum and incubated at  $37^{\circ}\text{C}$  for 30 min. The reaction was stopped by adding 0.5 mL of 2,4-dinitrophenylhydrazine (DNPH) reagent and allowed to stand for 20 min at room temperature. Subsequently, 5 mL of

0.4 mol/L NaOH solution was added to terminate the reaction and develop the color, and the absorbance was measured at 505 nm. Enzyme activities were expressed in U/L.

### ALP assays

ALP activity was determined using a colorimetric method based on the hydrolysis of p-nitrophenyl phosphate (pNPP). The reaction mixture consisted of 1.0 mL of buffered substrate solution (pH 10.4) and 0.02 mL of serum. After incubation at 37°C for 10 min, the reaction was terminated, and the formation of p-nitrophenol was measured at 405 nm. Enzyme activity was expressed in U/L.

### Bilirubin assays

Total bilirubin (TB) and direct bilirubin (DB) concentrations were determined using the diazo reaction method. Briefly, 0.2 mL of serum was mixed with 1.0 mL of diazo reagent (sulfanilic acid and sodium nitrite). For DB, the reaction proceeded in aqueous medium, whereas for TB, methanol was used as an accelerator to release albumin-bound bilirubin. After incubation for 10 min at room temperature, absorbance was measured at 540 nm. Results were expressed in mg/L. All assays were conducted in duplicate using a calibrated spectrophotometer, with reagent blanks included for each measurement to account for background absorbance.

### Liver tissue sampling and histological analysis

At the end of the experimental period (day 20), animals were weighed prior to sacrifice and then humanely euthanized by cervical dislocation. The liver was rapidly excised, rinsed in 0.9% NaCl solution, blotted dry, and weighed. Liver tissues were then fixed in 10% neutral buffered formalin for 24 h. Following fixation, the liver tissues were processed using standard histological procedures, including dehydration through a graded ethanol series, clearing, paraffin embedding, and sectioning at 5 µm thickness using a microtome. The sections were then mounted on glass slides, deparaffinized, rehydrated, and stained with hematoxylin and eosin (H&E). Histological examination was performed using a light microscope at different magnifications (4×, 10× and 40×) to evaluate liver architecture and

identify pathological alterations, including hepatocyte degeneration, inflammatory cell infiltration, necrosis, and structural disorganization. All histological analyses were conducted in accordance with standard protocols in a specialized pathology laboratory. For semi-quantitative histopathological evaluation, liver lesions were assessed microscopically by the investigators using a 4-grade severity scale: 0=absent, 1=mild, 2=moderate, and 3=severe, for each of the following parameters: hepatocyte ballooning, necrosis, inflammatory cell infiltration, and hepatocellular degeneration. The total histological injury score was calculated as the sum of individual lesion scores.

### Data analysis

The evolution of biochemical parameters across the 3 sampling times (T1, T2, and T3) is presented as the mean±SD and analyzed using the Kruskal-Wallis test. Data for body weight and relative liver weight were analyzed using descriptive statistics and are presented as mean±standard deviation, as well as minimum, first quartile, median, third quartile, and maximum values. The distribution of the data was visualized using box-and-whisker plots.

## RESULTS

All experimental groups remained clinically stable throughout the study period, with no mortality observed; however, animals in the paracetamol-treated group exhibited transient signs of toxicity, including reduced activity, piloerection, and mild respiratory distress within the first hours following intraperitoneal administration.

### Effect of paracetamol and *S. marianum* on biochemical parameters

#### ALT

At the first sampling (T1), highest activity was recorded in the control group (129.41±96.64 IU/L), followed by the paracetamol group (95.90±18.56 IU/L), while comparatively lower values were observed in the *S. marianum* group (62.48±24.50 IU/L) (Table 1). Alanine aminotransferase levels declined progressively from the second to the third sampling (T2 and T3) in all

**Table 1.** Alanine aminotransferase (ALT) (IU/L) activity in Wistar rats across different sampling times under various treatments

Sampling	Paracetamol	Paracetamol + <i>S. marianum</i>	<i>S. marianum</i>	Control	Treatment effect: $\chi^2=8.65$ $P=0.03^*$
1 <sup>st</sup> (T1)	95.90±18.56 <sup>b</sup>	77.41±11.46 <sup>ab</sup>	62.48±24.50 <sup>a</sup>	129.41±96.64 <sup>c</sup>	
2 <sup>nd</sup> (T2)	83.49±1.76 <sup>a</sup>	74.38±7.52 <sup>a</sup>	77.98±12.16 <sup>a</sup>	76.10±24.46 <sup>a</sup>	
3 <sup>rd</sup> (T3)	78.58±6.29 <sup>a</sup>	69.38±22.22 <sup>a</sup>	56.11±18.40 <sup>a</sup>	72.65±10.56 <sup>a</sup>	
<b>Sampling effect: <math>\chi^2=4.95</math>; <math>P=0.08</math></b>					

Data are presented as mean±SD (n=6); mean values followed by different uppercase letters indicate significant differences among treatments (Kruskal-Wallis test,  $P<0.05$ )

**Table 2.** Aspartate aminotransferase (AST) (IU/L) activity in Wistar rats across different sampling times under various treatments

Sampling	Paracetamol	Paracetamol + <i>S. marianum</i>	<i>S. marianum</i>	Control	Treatment effect: $\chi^2=5.05$ $P=0.17$
1 <sup>st</sup> (T1)	86.66±55.87 <sup>a</sup>	127.52±114.16 <sup>a</sup>	169.28±58.15 <sup>a</sup>	284.01±275.74 <sup>a</sup>	
2 <sup>nd</sup> (T2)	142.20±6.09 <sup>a</sup>	159.88±25.22 <sup>a</sup>	134.33±27.65 <sup>a</sup>	174.39±1.43 <sup>a</sup>	
3 <sup>rd</sup> (T3)	151.94±33.13 <sup>a</sup>	148.56±30.11 <sup>a</sup>	132.57±28.44 <sup>a</sup>	160.29±38.59 <sup>a</sup>	
<b>Sampling effect: <math>\chi^2=1.41</math>; <math>P=0.49</math></b>					

Data are presented as mean±SD (n=6); mean values followed by different uppercase letters indicate significant differences among treatments (Kruskal-Wallis test,  $P<0.05$ )

**Table 3.** Direct bilirubin (mg/L) levels in Wistar rats across different sampling times under various treatments

Sampling	Paracetamol	Paracetamol + <i>S. marianum</i>	<i>S. marianum</i>	Control	Treatment effect: $\chi^2=5.03$ $P=0.17$
1 <sup>st</sup> (T1)	10.42±7.68 <sup>a</sup>	1.59±0.42 <sup>a</sup>	2.32±1.22 <sup>a</sup>	9.82±6.97 <sup>a</sup>	
2 <sup>nd</sup> (T2)	2.12±0.76 <sup>a</sup>	3.23±1.00 <sup>a</sup>	2.55±1.17 <sup>a</sup>	2.48±1.08 <sup>a</sup>	
3 <sup>rd</sup> (T3)	1.89±0.57 <sup>a</sup>	2.65±1.35 <sup>a</sup>	1.79±0.68 <sup>a</sup>	2.85±1.38 <sup>a</sup>	
<b>Sampling effect: <math>\chi^2=3.71</math>; <math>P=0.16</math></b>					

Data are presented as mean±SD (n=6); mean values followed by different uppercase letters indicate significant differences among treatments (Kruskal-Wallis test,  $P<0.05$ )

groups, with the *S. marianum* group exhibiting the lowest values (77.98±12.16 to 56.11±18.40 IU/L) relative to the other treatments (Table 1). ALT activity was significantly influenced by treatment ( $\chi^2=8.65$ ,  $P=0.03$ ), while the effect of sampling time remained non-significant ( $\chi^2=4.95$ ,  $P=0.08$ ) (Table 1).

### AST

The control group showed markedly higher levels at the first sampling (T1) (284.01±275.74 IU/L) (Table 2), followed by the *S. marianum* group (169.28±58.15 IU/L) (Table 2). At the second and third samplings (T2 and T3), aspartate aminotransferase values became more homogeneous across all groups, ranging from 134.33±27.65 to 174.39±1.43 IU/L at the second sampling (T2) and from 132.57±28.44 to 160.29±38.59 IU/L at the third sampling (T3) (Table 2). However, no significant differences were observed between treatments ( $\chi^2=5.05$ ,  $P=0.17$ ) or sampling times ( $\chi^2=1.41$ ,  $P=0.49$ ) (Table 2).

### Effect on direct bilirubin

The results indicate that at the first sampling (T1), the paracetamol group showed higher direct bilirubin levels (10.42±7.68 mg/L) (Table 3), comparable to the control group (9.82±6.97 mg/L) (Table 3). In contrast, lower values were recorded in the *S. marianum* (2.32±1.22 mg/L). In the combined treatment group, lower values were observed (1.59±0.42 mg/L) (Table 3). At the second and third samplings (T2 and T3), DB levels decreased in all groups, with relatively similar values across treatments (Table 3). No significant differences were observed between treatments ( $\chi^2=5.03$ ,  $P=0.17$ ) or between sampling times ( $\chi^2=3.71$ ,  $P=0.16$ ) (Table 3).

### Effect on total bilirubin

Regarding total bilirubin, a significant treatment effect was detected ( $\chi^2=9.62$ ,  $P=0.02$ ), as well as a highly significant sampling effect ( $\chi^2=26.575$ ,  $P<0.001$ ) (Table 4). During the first sampling (T1), the control group

**Table 4.** Total bilirubin(mg/L) in Wistar rats across different sampling times under various treatments

Sampling	Paracetamol	Paracetamol + <i>S. marianum</i>	<i>S. marianum</i>	Control	Treatment effect $\chi^2=9.62$ $P=0.02^*$
1 <sup>st</sup> (T1)	14.69±7.42 <sup>b</sup>	5.20±0.45 <sup>a</sup>	7.31±2.72 <sup>ab</sup>	30.62±23.73 <sup>c</sup>	
2 <sup>nd</sup> (T2)	5.18±0.40 <sup>a</sup>	5.52±0.59 <sup>a</sup>	5.00±0.58 <sup>a</sup>	6.35±0.45 <sup>a</sup>	
3 <sup>rd</sup> (T3)	4.07±0.72 <sup>a</sup>	5.70±1.72 <sup>a</sup>	4.28±0.49 <sup>a</sup>	5.08±1.63 <sup>a</sup>	
Sampling effect: $\chi^2=26.575$ ; $P<0.001^{***}$					

[Data are presented as mean±SD (n=6). Mean values followed by different uppercase letters indicate significant differences among treatments (Kruskal-Wallis test,  $P<0.05$ )]

**Table 5.** Alkaline phosphatase (ALP) (IU/L) activity in Wistar rats across different sampling times under various treatments

Sampling	Paracetamol	Paracetamol + <i>S. marianum</i>	<i>S. marianum</i>	Control	Treatment effect: $\chi^2 = 9.58$ $P = 0.02^*$
1 <sup>st</sup> (T1)	542.46±36.03 <sup>a</sup>	473.86±107.14 <sup>a</sup>	486.04±88.64 <sup>a</sup>	495.97±54.50 <sup>a</sup>	
2 <sup>nd</sup> (T2)	607.34±39.64 <sup>a</sup>	593.12±150.23 <sup>a</sup>	546.92±91.69 <sup>a</sup>	559.34±32.12 <sup>a</sup>	
3 <sup>rd</sup> (T3)	593.23±76.08 <sup>a</sup>	422.83±155.09 <sup>b</sup>	408.03±140.23 <sup>b</sup>	514.08±122.73 <sup>ab</sup>	
Sampling effect: $\chi^2 = 8.24$ ; $P = 0.02^*$					

Data are presented as mean±SD (n=6); mean values followed by different uppercase letters indicate significant differences among treatments (Kruskal-Wallis test,  $P<0.05$ )

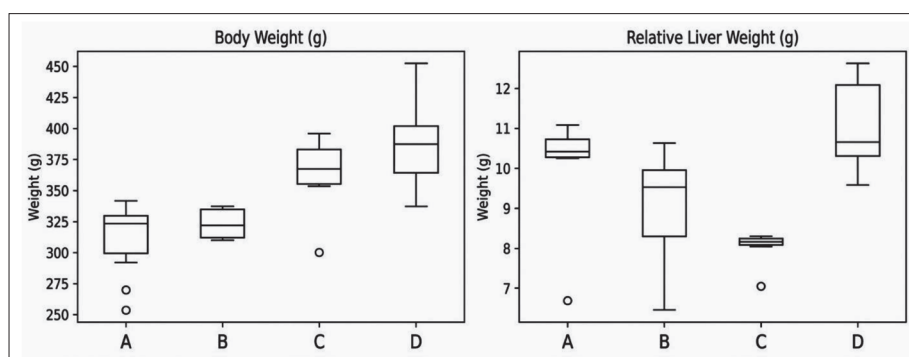


**Fig. 1.** Distribution of body weight and relative liver weight in Wistar rats across experimental groups; A – paracetamol; B – paracetamol + *S. marianum*; C – *S. marianum*; D – control.

showed the highest TB level (30.62±23.73 mg/L) (Table 4), followed by the paracetamol group (14.69±7.42 mg/L) (Table 2), while lower values were recorded in the combined (5.20±0.45 mg/L) and *S. marianum* groups (7.31±2.72 mg/L) (Table 2). At the second and third samplings (T2 and T3), TB levels substantially declined and stabilized across all groups (Table 4).

### ALP

Alkaline phosphatase levels were significantly affected by treatment ( $\chi^2=9.58$ ,  $P=0.02$ ) and sampling time ( $\chi^2=8.24$ ,  $P=0.02$ ) (Table 5). At the first sampling (T1), ALP values were relatively comparable between groups, with slightly higher levels in the paracetamol group (542.46±36.03 IU/L). At the second sampling (T2), an

increase was observed in all groups, particularly in the paracetamol group (607.34±39.64 IU/L). At the third sampling (T3), a decrease was noted in the *S. marianum* and combined treatment groups, suggesting a possible protective or regulatory effect.

### Effect of paracetamol and *S. marianum* on body and liver weights in Wistar rats:

Fig. 1 presents the box-and-whisker plots illustrating the distribution of body weight and relative liver weight across the experimental groups. Our results show that body weight exhibited a progressive increase across groups, ranging from a median of 323.5 g in the paracetamol group to 387.5 g in the control group (Fig. 1), with intermediate values observed in

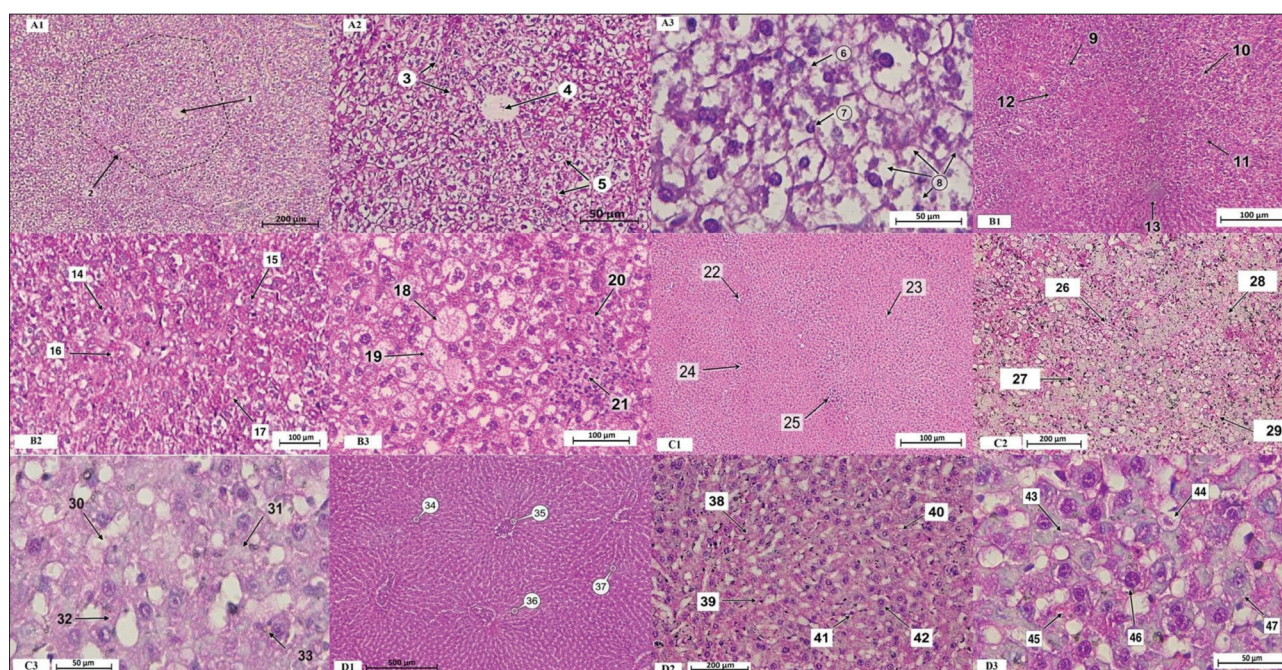


**Fig. 2.** Histopathological assessment of liver tissue following paracetamol and *S. marianum* treatments. Images were captured at different magnifications (4x), (10x) and (40x). Control group: A1: (4x); 1: Central vein; 2: Hepatic lobule; A2: (10x); 3: Hepatocyte cords; 4: Central vein; 5: Hepatic sinusoids; A3: (40x); 6: Hepatocyte; 7: Nucleus; 8: Hepatic sinusoid. Paracetamol group: B1: (4x); 9: Hepatocyte ballooning; 10: Necrotic area; 11: Inflammatory cell infiltration; 12: Hepatocyte degeneration; 13: Central vein; B2: (10x); 14: Hepatocyte ballooning; 15: Necrotic area; 16: Hepatocyte degeneration; 17: Inflammatory cell infiltration; B3: (40x); 18: Hepatocyte ballooning; 19: Hepatocyte degeneration; 20: Necrotic area; 21: Inflammatory cell infiltration. Paracetamol + *S. marianum* group: C1: (4x); 22: Hepatocyte ballooning (mild); 23: Necrotic area (mild); 24: Hepatocyte degeneration (mild); 25: Inflammatory cell infiltration (mild); C2: (10x); 26: Hepatocyte ballooning (mild); 27: Hepatocyte degeneration (mild); 28: Necrotic area (mild); 29: Inflammatory cell infiltration (mild); C3: (40x); 30: Hepatocyte ballooning (mild); 31: Necrotic area (mild); 32: Hepatocyte degeneration (mild); 33: Inflammatory cell infiltration (mild). *S. marianum* group: D1: (4x); 34: Hepatocytes well organized in regular cords; 35: Central vein (normal); 36: Portal triad (normal); 37: Sinusoids (normal); D2: (10x); 38: Hepatocytes well organized in regular cords; 39: Hepatocyte degeneration (absent); 40: Sinusoids (normal); 41: Nuclei normal, regular in appearance; 42: Cytoplasm homogeneous and mostly non-vacuolated; D3: (4x); 43: Hepatocytes well organized in regular cords; 44: Sinusoids (normal); 45: Cytoplasm homogeneous and mostly non-vacuolated; 46: Nuclei normal, regular in appearance; 47: Hepatocyte degeneration (absent).

the paracetamol + *S. marianum* group (median: 323.5 g; mean:  $321.7 \pm 11.9$  g) and higher values in the *S. marianum* group (median: 376.5 g; mean:  $361.7 \pm 37.6$  g). A similar pattern was observed for relative liver weight, with the lowest median values recorded in the *S. marianum* group (8.20 g; mean:  $8.00 \pm 0.45$  g), intermediate values in the paracetamol + *S. marianum* and paracetamol groups (medians: 9.54 g and 10.41 g, respectively), and the highest values observed in the control group (median: 10.66 g; mean:  $10.94 \pm 1.03$  g).

### Effect of paracetamol and *S. marianum* on liver histology

Representative photomicrographs of H&E-stained liver sections from different experimental groups are

presented. The control group showing normal hepatic architecture with well-preserved lobular organization around the central vein, regularly arranged hepatocyte cords, intact hepatic sinusoids, and morphologically normal hepatocytes with clear nuclei and homogeneous cytoplasm (Figs. 2A1, A2, and A3). The paracetamol group showed marked histopathological alterations indicative of severe hepatotoxicity, including hepatocyte ballooning, extensive necrotic areas, pronounced cellular degeneration, and inflammatory cell infiltration, reflecting a significant disruption of hepatic tissue architecture (Figs. 2B1, B2, and B3).

The paracetamol + *S. marianum* group demonstrated partial histological improvement, characterized by mild hepatocyte ballooning, reduced necrosis, moderate cellular degeneration, and decreased inflammatory

**Table 6.** Semi-quantitative histopathological lesion scoring in liver tissue

Group	Ballooning	Necrosis	Inflammation	Degeneration	Total score
Control	0	0	0	0	0
Paracetamol	3	3	2	3	11
Paracetamol + <i>S. marianum</i>	1	1	1	2	5
<i>S. marianum</i>	0	0	0	0	0

Data are presented as semi-quantitative histopathological lesion scores based on microscopic evaluation using a 4-grade severity scale (0=absent, 1=mild, 2=moderate, 3=severe). Total score represents the sum of individual lesion scores.

infiltration, suggesting a protective but incomplete ameliorative effect of *S. marianum* (Figs. 2C1, C2 and C3). *S. marianum* group showed a preserved and well-organized hepatic structure comparable to the control group, with regularly arranged hepatocyte cords, normal central vein and portal triads, intact sinusoids, homogeneous cytoplasm, and absence of hepatocyte degeneration or necrosis, indicating the non-toxic and hepatoprotective nature of the plant (Fig. 2D1, D2 and D3).

Semi-quantitative lesion scoring confirmed the histological observations (Table 6). The paracetamol group exhibited the highest total histological injury score, characterized by severe ballooning, necrosis, inflammatory infiltration, and hepatocellular degeneration (total score=11). In contrast, the paracetamol + *S. marianum* group showed a markedly reduced lesion severity (total score=5), whereas the control and *S. marianum*-alone groups showed no significant histological lesions (Table 6).

## DISCUSSION

Our study evaluated the impact of acute paracetamol exposure on hepatic integrity and the potential protective role of *S. marianum* in Wistar rats. The results suggest a relative divergence between histological alterations and biochemical responses under the present experimental conditions, with paracetamol inducing pronounced structural liver injury, while serum biomarkers showed only moderate or inconsistent alterations. This observation represents an important contribution of the present work because it shows that conventional circulating biomarkers alone may underestimate the severity of acute hepatocellular injury when assessed outside peak necrotic windows, whereas tissue-level evaluation reveals persistent and biologically meaningful structural damage. The absence of significant body

and liver weight alterations further suggests that the experimental model induced localized hepatic injury without systemic cachexia or severe metabolic disruption, which is typical of acute paracetamol exposure rather than chronic toxicity [20,23,26].

In the present study, ALT and AST levels were not significantly altered, except for a modest treatment effect on ALT, whereas AST remained unchanged. This pattern suggests that biochemical leakage of aminotransferases was limited or temporally delayed [21,22,39]. Such discrepancies between enzyme activity and tissue damage have been previously reported in early or subacute stages of paracetamol toxicity, where mitochondrial injury [23,24,30] and centrilobular necrosis may precede sustained enzyme elevation [29,32]. More recent studies also suggest that ALT and AST levels may not fully reflect the extent of hepatocellular injury when sampling is performed outside peak necrotic phases or when compensatory detoxification pathways remain partially functional [22,27,28,39]. Importantly, our findings experimentally reinforce this concept by directly demonstrating, in the same biological model, that biochemical stability does not necessarily mean histological preservation. This integrated observation strengthens the argument for combining serum biomarkers with tissue-based evaluation in experimental hepatotoxicity studies. These effects are consistent with the well-established mechanisms described in the literature for paracetamol-induced liver injury involving CYP450-dependent metabolism and downstream mitochondrial dysfunction [6-8,16,17,23,30,32].

Histopathological analysis provided clear evidence of hepatotoxicity, including hepatocyte ballooning, necrosis, inflammatory infiltration, and architectural disorganization. This result is consistent with those reported in [29], where paracetamol administration induced marked centrilobular hepatocellular necrosis

and progressive histopathological damage, confirming the strong hepatotoxic potential of this drug. The marked structural alterations observed despite moderate biochemical changes suggest that histological analysis may provide additional sensitivity in detecting hepatic injury under the present experimental conditions. Moreover, the incorporation of a semi-quantitative histological scoring approach in the present study constitutes a methodological strength, allowing objective grading of tissue lesions and a more robust comparison between untreated and treated groups. This quantitative histological dimension increases the translational value of the experimental findings.

The semi-quantitative histological scoring further strengthened these observations by objectively confirming the marked severity of lesions in the paracetamol group and their attenuation following *S. marianum* treatment. This attenuation occurred even in the absence of complete normalization of serum biochemical parameters, suggesting that tissue recovery mechanisms may precede or exceed detectable systemic biochemical correction. This temporal dissociation further supports the hypothesis that structural hepatic recovery may precede complete biochemical normalization in acute toxic injury.

Regarding bilirubin metabolism, total bilirubin showed a significant effect of treatment and sampling time, whereas direct bilirubin remained non-significant. The transient elevation of TB at T1 in the paracetamol group reflects early impairment of hepatic excretory function, likely associated with hepatocellular dysfunction rather than true cholestasis. Similar transient bilirubin fluctuations have been reported in acute toxic injury models, where bile transport systems are secondarily affected by oxidative stress and membrane disruption [32-36]. The subsequent normalization across groups suggests activation of compensatory hepatic clearance mechanisms during recovery. Our results align with [36], who emphasizes the protective role of bilirubin as an endogenous antioxidant in limiting oxidative liver damage.

Alkaline phosphatase (ALP) displayed a significant treatment and sampling effect, with a marked increase at T2 followed by partial normalization at T3 in the *S. marianum*-treated groups. This dynamic profile suggests a transient cholestatic or membrane instability phase followed by recovery. Recent hepatotoxicity

models indicate that ALP is particularly sensitive to membrane phospholipid perturbation and canalicular transport dysfunction [33,38,39]. Importantly, *S. marianum* induced a consistent histological improvement despite limited biochemical normalization, particularly in ALT/AST and bilirubin parameters. Liver sections from treated groups showed reduced necrosis and improved hepatic architecture, confirming a cytoprotective effect. The partial discrepancy between histological improvement and biochemical normalization suggests that *S. marianum* may exert its hepatoprotective effects primarily through membrane stabilization and attenuation of cellular damage rather than through complete normalization of serum enzyme levels under acute injury conditions [12-15,37,40-42]. These observations suggest that the hepatoprotective action of *S. marianum* in acute toxic injury may primarily involve preservation of cellular architecture, stabilization of membrane integrity, and attenuation of tissue necrosis, rather than immediate normalization of conventional serum biomarkers. From a translational perspective, this finding indicates that therapeutic efficacy may be underestimated when evaluation relies exclusively on circulating biochemical indicators.

While the study by Mukhtar et al. [40] demonstrated that encapsulated silymarin improves bioavailability and effectively attenuates paracetamol-induced hepatic injury through reductions in liver enzymes and oxidative stress markers, our study provides additional insight by highlighting the histopathological dimension of hepatoprotection, showing that *S. marianum* not only modulates biochemical parameters but also partially preserves liver architecture under acute toxic conditions, thereby emphasizing its functional relevance beyond pharmacotechnological optimization.

To our knowledge, few experimental studies have simultaneously integrated longitudinal biochemical monitoring, semi-quantitative histopathological scoring, and therapeutic evaluation of *S. marianum* within the same acute paracetamol-induced hepatotoxicity model. One distinctive strength of the present study lies in this integrative framework, which provides a more comprehensive understanding of hepatoprotection than approaches based solely on circulating biomarkers. However, some limitations should be acknowledged, including the relatively small sample size and the absence of direct quantification of oxidative stress biomarkers, inflammatory mediators, or

molecular signaling pathways that could further clarify the mechanistic basis of hepatoprotection. Future studies incorporating biochemical, histological, and molecular endpoints would strengthen translational interpretation of these findings. The present study provides mechanistic and histopathological evidence by demonstrating that the protective effects of *S. marianum* extend beyond biochemical modulation and include measurable preservation of hepatic microarchitecture. This constitutes the principal added value of our work and supports combined morphological and biochemical assessment as a robust experimental framework for future hepatoprotective and toxicological investigations.

## CONCLUSION

Acute paracetamol administration induced marked hepatocellular injury in Wistar rats, characterized by severe histopathological alterations including hepatocyte ballooning, necrosis, inflammatory infiltration, and disruption of hepatic architecture. These structural lesions were more pronounced than the associated biochemical disturbances, indicating that histopathological examination may provide greater sensitivity than serum liver biomarkers alone for detecting acute hepatic injury. This dissociation between tissue injury and circulating biochemical markers underscores the importance of integrated assessment strategies for accurately characterizing acute hepatotoxicity. Treatment with *Silybum marianum* partially attenuated paracetamol-induced liver damage, improving hepatic tissue organization and reducing the severity of necrotic and inflammatory changes. Although biochemical recovery remained moderate, the histological improvement supports the hepatoprotective potential of *S. marianum*, likely through antioxidant, anti-inflammatory, and membrane-stabilizing mechanisms. Notably, the observed preservation of hepatic microarchitecture despite incomplete biochemical normalization suggests that structural recovery may precede measurable systemic biochemical correction during the healing process. Overall, these findings support the value of combining biochemical and histopathological approaches in experimental hepatotoxicity studies and present *S. marianum* as a promising natural hepatoprotective agent. More broadly, the present work demonstrates that integrated morphological and biochemical evaluation

constitutes a robust experimental framework for future investigations of hepatoprotective therapies and toxic liver injury mechanisms.

**Funding:** The authors received no specific funding for this work.

**Author contributions:** AF: conceptualization, investigation, methodology, formal analysis, software, data curation and writing the manuscript. WH: software, data analysis and writing the manuscript. HF: proposed the subject, supervision, study design, scientific advice and review. The final version was reviewed and approved by all authors.

**Conflict of interest disclosure:** The authors declare no conflicts of interest.

**Data availability:** The data supporting this article are available in the online dataset: <https://figshare.com/s/db9ab8a732c255e18bc7> and <https://figshare.com/s/3d8667c0d5268632a347> (Dunn post-hoc-Bonferroni)

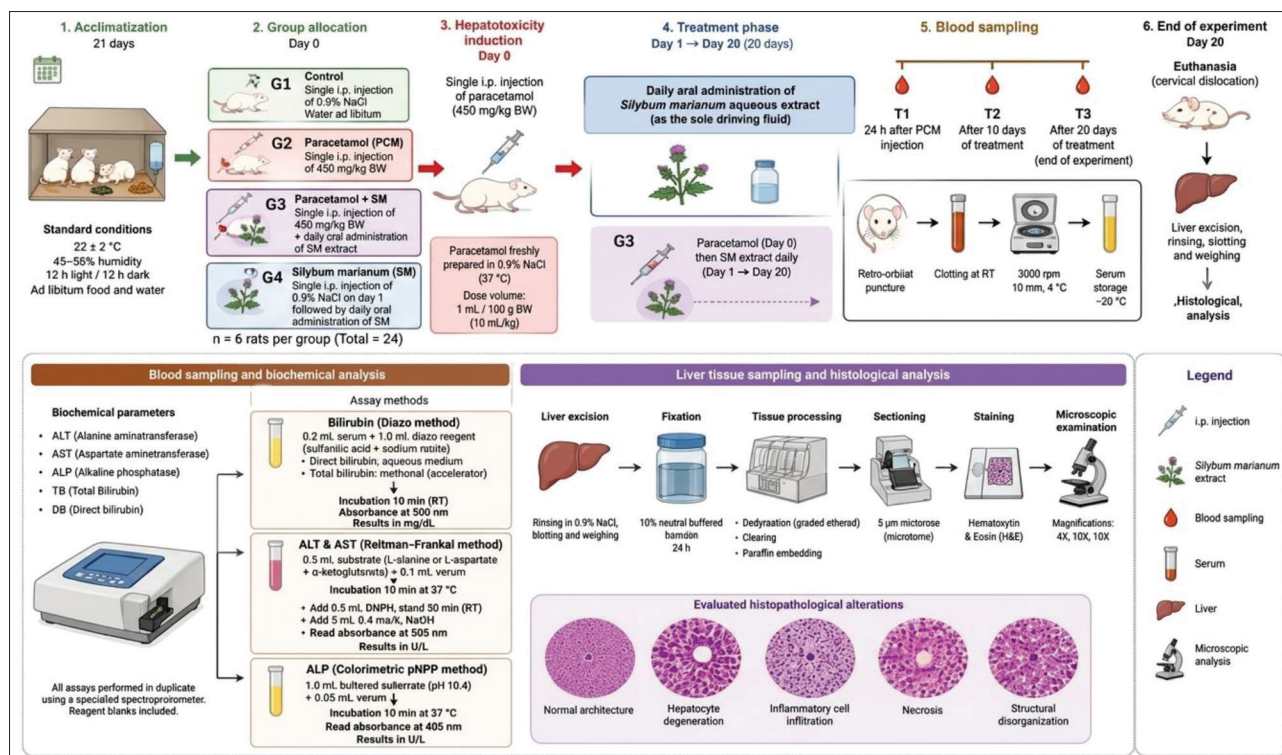
## REFERENCES

1. Ramachandran A, Jaeschke H. Mechanisms of acetaminophen hepatotoxicity and their translation to the human pathophysiology. *J Clin Transl Res*. 2017;3(1):157-69. <https://doi.org/10.18053/jctres.03.2017S1.002>
2. McGill MR, Jaeschke H. Mechanistic biomarkers in acetaminophen-induced hepatotoxicity and acute liver failure: from preclinical models to patients. *Expert Opin Drug Metab Toxicol*. 2014;10(7):1005-17. <https://doi.org/10.1517/17425255.2014.918101>
3. Jaeschke H, Ramachandran A. Oxidant stress and lipid peroxidation in acetaminophen hepatotoxicity. *React Oxyg Species*. 2018;5(15):145-58. <https://doi.org/10.20455/ros.2018.807>
4. Lee WM. Acetaminophen (APAP) hepatotoxicity—Isn't it time for APAP to go away? *J Hepatol*. 2017;67(6):1324-31. <https://doi.org/10.1016/j.jhep.2017.07.005>
5. Yoon E, Babar A, Choudhary M, Kutner M, Prysopoulos N. Acetaminophen-induced hepatotoxicity: a comprehensive update. *J Clin Transl Hepatol*. 2016;4(2):131-42. <https://doi.org/10.14218/JCTH.2015.00052>
6. McGill MR, Jaeschke H. Metabolism and disposition of acetaminophen: recent advances in relation to hepatotoxicity and diagnosis. *Pharm Res*. 2013;30(9):2174-87. <https://doi.org/10.1007/s11095-013-1007-6>
7. McGill MR, Sharpe MR, Williams CD, Taha M, Curry SC, Jaeschke H. The mechanism underlying acetaminophen-induced hepatotoxicity in humans and mice involves mitochondrial damage and nuclear DNA fragmentation. *J Clin Invest*. 2012;122(4):1574-83. <https://doi.org/10.1172/JCI59755>
8. Kon K, Kim JS, Jaeschke H, Lemasters JJ. Mitochondrial permeability transition in acetaminophen-induced necrosis and apoptosis of cultured mouse hepatocytes. *Hepatology*. 2004;40(5):1170-79. <https://doi.org/10.1002/hep.20437>

9. Ju C, Reilly TP, Bourdi M, Radonovich MF, Brady JN, George JW, Pohl LR. Protective role of Kupffer cells in acetaminophen-induced hepatic injury in mice. *Chem Res Toxicol.* 2002;15(12):1504-13. <https://doi.org/10.1021/tx0255976>
10. Woolbright BL, Jaeschke H. Role of the inflammasome in acetaminophen-induced liver injury and acute liver failure. *J Hepatol.* 2017;66(4):836-48. <https://doi.org/10.1016/j.jhep.2016.11.017>
11. Antoine DJ, Williams DP, Kipar A, Jenkins RE, Regan SL, Sathish JG, Park BK. High-mobility group box-1 protein and keratin-18, circulating serum proteins informative of acetaminophen-induced necrosis and inflammation in acute liver injury. *Toxicol Sci.* 2009;112(2):521-31. <https://doi.org/10.1093/toxsci/kfp200>
12. Abenavoli L, Capasso R, Milic N, Capasso F. Milk thistle in liver diseases: past, present, future. *Phytother Res.* 2010;24(10):1423-32. <https://doi.org/10.1002/ptr.3207>
13. Federico A, Dallio M, Loguercio C. Silymarin/Silybin and Chronic Liver Disease: A Marriage of Many Years. *Molecules.* 2017;22(2):191. <https://doi.org/10.3390/molecules22020191>
14. Vargas-Mendoza N, Madrigal-Santillán E, Morales-González Á, Esquivel-Soto J, Esquivel-Chirino C, García-Luna y González-Rubio M, Gayosso-de-Lucio JA, Morales-González JA. Hepatoprotective effect of silymarin. *World J Hepatol.* 2014;6(3):144-9. <https://doi.org/10.4254/wjh.v6.i3.144>
15. Gillessen A, Schmidt HHJ. Silymarin as Supportive Treatment in Liver Diseases: A Narrative Review. *Adv Ther.* 2020;37(4):1279-301. <https://doi.org/10.1007/s12325-020-01251-y>
16. Hinson JA, Roberts DW, James LP. Mechanisms of Acetaminophen-Induced Liver Necrosis. *Handb Exp Pharmacol.* 2010;196:369-405. [https://doi.org/10.1007/978-3-642-00663-0\\_12](https://doi.org/10.1007/978-3-642-00663-0_12)
17. Jaeschke H, McGill MR, Ramachandran A. Oxidant stress, mitochondria, and cell death mechanisms in drug-induced liver injury: lessons learned from acetaminophen hepatotoxicity. *Drug Metab Rev.* 2012;44(1):88-106. <https://doi.org/10.3109/03602532.2011.602688>
18. Polyak SJ, Morishima C, Lohmann V, Pal S, Lee DYW, Liu Y, Graf TN, Oberlies NH. Identification of hepatoprotective flavonolignans from silymarin. *Proceedings of the National Academy of Sciences of the United States of America.* 2010;107(13):5995-9. <https://doi.org/10.1073/pnas.0914009107>
19. Reitman S, Frankel S. A colorimetric method for the determination of serum glutamic oxalacetic and glutamic pyruvic transaminases. *Am J Clin Path.* 1957;28(1):56-63. <https://doi.org/10.1093/ajcp/28.1.56>
20. Izawa T, Travlos GS, Cortes RA, Clayton NP, Sills RC, Pandiri AR. Absence of Increased Susceptibility to Acetaminophen-Induced Liver Injury in a Diet-Induced NAFLD Mouse Model. *Toxicol Pathol.* 2023;51(3):112-25. <https://doi.org/10.1177/01926233231171101>
21. Giannini EG. Liver enzyme alteration: A guide for clinicians. *C M A J.* 2005;172(3):367-79. <https://doi.org/10.1503/cmaj.1040752>
22. McGill MR. The past and present of serum aminotransferases and the future of liver injury biomarkers. *EXCLI J.* 2016;15:817. <https://doi.org/10.17179/EXCLI2016-800>
23. Ramachandran A, Jaeschke H. Acetaminophen Hepatotoxicity—A Mitochondrial Perspective. *Adv Pharmacol.* 2019;85:195-219. <https://doi.org/10.1016/bs.apha.2019.01.007>
24. Dunn KW, Martinez MM, Wang Z, Mang HE, Clendenon SG, Sluka JP, Glazier JA, Klaunig JE. Mitochondrial depolarization and repolarization in the early stages of acetaminophen hepatotoxicity in mice. *Toxicology.* 2020;439:152464. <https://doi.org/10.1016/j.tox.2020.152464>
25. McGill MR, Jaeschke H. Metabolism and disposition of acetaminophen: recent advances in relation to hepatotoxicity and diagnosis. *Pharm Res.* 2013;30(9):2174-87. <https://doi.org/10.1007/s11095-013-1007-6>
26. Rotundo L, Pysopoulos N. Liver injury induced by paracetamol and challenges associated with intentional and unintentional use. *World J Hepatol.* 2020;12(4):125-36. <https://doi.org/10.4254/wjh.v12.i4.125>
27. Dufour DR, Lott JA, Nolte FS, Gretch DR, Koff RS, Seeff LB. Diagnosis and monitoring of hepatic injury. II. Recommendations for use of laboratory tests in screening, diagnosis, and monitoring. *Clin Chem.* 2000;46(12):2050-68. <https://doi.org/10.1093/clinchem/46.12.2050>
28. Kalas MA, Chavez L, Leon M, Taweedsed PT, Surani S. Abnormal liver enzymes: A review for clinicians. *World J Hepatol.* 2021;13(11):1688-98. <https://doi.org/10.4254/wjh.v13.i11.1688>
29. Muhammad-Azam F, Nur-Fazila SH, Ain-Fatin R, Mustapha Noordin M, Yimer N. Histopathological changes of acetaminophen-induced liver injury and subsequent liver regeneration in BALB/C and ICR mice. *Vet World.* 2019;12(11):1682-8. <https://doi.org/10.14202/vetworld.2019.1682-1688>
30. Jaeschke H, Duan L, Nguyen NT, Ramachandran A. Mitochondrial damage and biogenesis in acetaminophen-induced liver injury. *Liver Res.* 2019;3(3-4):150-6. <https://doi.org/10.1016/j.livres.2019.10.002>
31. Du K, Ramachandran A, Jaeschke H. Oxidative stress during acetaminophen hepatotoxicity: Sources, pathophysiological role and therapeutic potential. *Redox Biol.* 2016;10:148-56. <https://doi.org/10.1016/j.redox.2016.10.001>
32. Li R, Wu H, Xu Y, Xu X, Xu Y, Huang H, Lv X, Liao C, Ye J, Li H. Underlying mechanisms and treatment of acetaminophen induced liver injury (Review). *Mol Med Rep.* 2025;31(4):1-13. <https://doi.org/10.3892/mmr.2025.13471>
33. Roma MG, Sanchez Pozzi EJ. Oxidative stress: A radical way to stop making bile. *Ann Hepatol.* 2008; 7(1): 16-33. [https://doi.org/10.1016/S1665-2681\(19\)31884-8](https://doi.org/10.1016/S1665-2681(19)31884-8)
34. Chen Z, Vong CT, Gao C, Chen S, Wu X, Wang S, Wang Y. Bilirubin Nanomedicines for the Treatment of Reactive Oxygen Species (ROS)-Mediated Diseases. *Mol Pharm.* 2020;17(7):2260-74. <https://doi.org/10.1021/acs.molpharmaceut.0c00337>
35. Ramírez-Mejía MM, Castillo-Castañeda SM, Pal SC, Qi X, Méndez-Sánchez N. The Multifaceted Role of Bilirubin in Liver Disease: A Literature Review. *J Clin Transl Hepatol.* 2024;12(11):939-48. <https://doi.org/10.14218/JCTH.2024.00156>

36. Martín PL, Hillotte GL, Razori MV, Massa EMA, Martínez AI, Del Luján Corbo M, Sánchez Pozzi EJ, Crocenzi FA, Roma MG, Basiglio CL. Inhibition of Bilirubin Generation Exacerbates Oxidative Stress and Liver Injury in Early to Intermediate Obstructive Cholestasis. *Clin Exp Pharmacol Physiol.* 2026; 53(4):e70123. <https://doi.org/10.1111/1440-1681.70123>
37. Bahmani M, Shirzad H, Rafieian S, Rafieian-Kopaei M. *Silybum marianum*: Beyond Hepatoprotection. *J Evid-Based Complementary Altern Med.* 2015;20(4):292-01. <https://doi.org/10.1177/2156587215571116>
38. Levitt MD, Hapak SM, Levitt DG. Alkaline Phosphatase Pathophysiology with Emphasis on the Seldom-Discussed Role of Defective Elimination in Unexplained Elevations of Serum ALP - A Case Report and Literature Review. *Clin Exp Gastroenterol.* 2022;15:41-9. <https://doi.org/10.2147/CEG.S345531>
39. Metri S, Rasamallu R, Mathew C, Mudunuri GR, Mohammad S. Comprehensive Review on Biomarkers in Hepato-toxicity: From Conventional Indicators to Omics Driven Discoveries. *Biosc Biotechnol Res Asia.* 2025; 22(3):3412. <https://doi.org/10.13005/bbra/3412>
40. Mukhtar S, Xiaoxiong Z, Qamer S, Saad M, Mubarak MS, Mahmoud AH, Mohammed OB. Hepatoprotective activity of silymarin encapsulation against hepatic damage in albino rats. *Saudi J Biol Sci.* 2021;28(1):717-23. <https://doi.org/10.1016/j.sjbs.2020.10.063>
41. Yang W, Liang Z, Wen C, Jiang X, Wang L. Silymarin Protects against Acute Liver Injury Induced by Acetaminophen by Downregulating the Expression and Activity of the CYP2E1 Enzyme. *Molecules (Basel, Switzerland).* 2022; 27(24):8855. <https://doi.org/10.3390/molecules27248855>
42. Jaffar HM, Al Asmari F, Khan FA, Rahim MA, Zongo E. Silymarin: Unveiling its pharmacological spectrum and therapeutic potential in liver diseases—A comprehensive narrative review. *Food Sci Nutr.* 2024; 12(5):3097-111. <https://doi.org/10.1002/fsn3.4010>

## SUPPLEMENTARY MATERIALS



**Supplementary Fig. S1.** Schematic diagram of the experimental design and timeline of paracetamol-induced hepatotoxicity and *S. marianum* treatment in rats, including group allocation, blood sampling, and liver histological analysis.